JOURNAL OF MATERIALS SCIENCE: MATERIALS IN MEDICINE 13 (2002) 485–489

Correlation between structure and compressive strength in a reticulated glass-reinforced hydroxyapatite foam

S. CALLCUT, J. C. KNOWLES*
Department of Biomaterials, Eastman Dental Institute, University College London, 256 Gray's Inn Road, London, WC1X 8LD, UK
E-mail: j.knowles@eastman.ucl.ac.uk

Glass-reinforced hydroxyapatite (HA) foams were produced using reticulated foam technology using a polyurethane template with two different pore size distributions. The mechanical properties were evaluated and the structure analyzed through density measurements, image analysis, X-ray diffraction (XRD) and scanning electron microscopy (SEM). For the mechanical properties, the use of a glass significantly improved the ultimate compressive strength (UCS) as did the use of a second coating. All the samples tested showed the classic three regions characteristic of an elastic brittle foam. From the density measurements, after application of a correction to compensate for the closed porosity, the bulk and apparent density showed a 1 : 1 correlation. When relative bulk density was plotted against UCS, a non-linear relationship was found characteristic of an isotropic open celled material.

It was found by image analysis that the pore size distribution did not change and there was no degradation of the macrostructure when replicating the ceramic from the initial polyurethane template during processing. However, the pore size distributions did shift to a lower size by about 0.5 mm due to the firing process. The ceramic foams were found to exhibit mechanical properties typical of isotropic open cellular foams.

Introduction

Hydroxyapatite (HA) is used extensively and in many forms for bone implants due to its high biocompatibility and its similarity in composition to the apatite found in natural bone. Porous HA can be used as a bone filler and although the mechanical properties are poor because of the high porosity required, the ability for the penetration of bone into the implant will lead to a secure, mechanically stable, integrated implant [1].

Preparation of porous HA to date has included the use of defatted and sterile bovine bone [2] the hydrothermal conversion of coral to HA [3], burn out methods using poly vinyl butyral particles [4] and foaming methods [5]. However, controlling the pore size and interconnectivity in the burn out and foaming methods and controlling impurities in bovine and coral sources can pose a problem. A novel route found for the preparation of reticulated porous HA has involved the use of reticulated foam technology [6, 7], where a polyurethane template is infiltrated with a ceramic slurry, left to dry and then the polyurethane burnt off to leave a ceramic replica of the polyurethane.

When preparing porous HA through the use of reticulated foam technology it is important that the template is copied exactly so that the porosity and interconnectivity can be controlled as the morphology of the porous implants is very important to obtain good implant incorporation. A minimum pore size of 100–150 μm is often suggested to achieve good implant fixation through bone ingrowth. It has also been proposed that lower density porous HA present a better implant material for the filling of osseous defects as a result of faster rate of osseointegration, which therefore leads to enhanced mechanical properties *in vivo* [8]. Open or reticulated porosity is also an important factor to be considered when characterizing the macroporous structure [1].

Gibson *et al*. [9] have successfully predicted the behavior of cellular solids and highly porous materials, classifying them as either open or closed cell models. Mechanical properties of low-density structures such as porous ceramics and cancellous bone can be modeled to their relative density by the following equation [9]:

$$\sigma = c_1 \left(\frac{\rho}{\rho^*} \right)^x$$

where σ is the ultimate compressive strength and ρ/ρ^* the relative density. x equals 2 in an open celled isotropic foam, and x equals 1 for a closed cell isotropic foam. c_1 is

*Author to whom all correspondence should be addressed.

the proportionality constant and is dependant on the structure of the strut material; it has therefore been found to be reduced when porosity is present within the ceramic struts [10].

Materials and methods

The HA used to prepare both the unreinforced and the glass-reinforced HA (GR-HA) foams was supplied by Plasma Biotal (Batch P120, Plasma Biotal, Derbyshire, UK). The glass was prepared from precursors of NaH_2PO_4 (37.2 g), $CaCO_3$ (41 g) and P_2O_5 (41.95 g). These components were thoroughly mixed and then poured into a Pt/10%Rh crucible which was then placed in a Carbolite furnace at 1200 °C for 2 h. After 2 h, the crucible was removed and the glass poured onto a steel plate to give a glass with the composition 15 mol % Na_2O, 40 mol % CaO, 45 mol % P_2O_5.

The production of these slips has been detailed elsewhere [7], but briefly to make a glass-reinforced slip, 2 g of the glass was dry ball milled for 24 h and then 98 g of HA was added and 150 ml of methanol as a suspending medium and wet milled for a further 24 h. The slip was poured out and then the methanol removed by drying at 80 °C. The HA powder was prepared in exactly the same way but without the initial glass stage. The porous HA and GR-HA samples were prepared by resuspending the appropriate powder in water [7] and immersing a polyurethane foam template (Customs Foam Ltd.) of known porosity into a rheologically optimized HA or GR-HA slip. The excess slip was squeezed out and the ceramic-coated foam was then fired at $1\,^{\circ}C\,min^{-1}$ to 600 °C to slowly burn off the polyurethane foam and then at $5\,^{\circ}C\,min^{-1}$ to 1250 °C and held for 8 h to fully sinter the ceramic. This gave a porous HA or GR-HA ceramic with the identical macrostructure as the polyurethane. To create a foam with better mechanical properties the foams could be coated with a second layer of the ceramic slip. The slip used was as above and the sintered ceramics were immersed in this slip for 15 s, which allowed the slip to penetrate the pores. The ceramic foam was then removed and the excess slip blown off with compressed air to ensure complete reticulation. The ceramics were allowed to dry for 24 h before firing using the same firing schedule as with the first firing.

Image analysis

Image analysis was used to determine the pore dimensions and distributions of two foams with different porosity's before and after coating in ceramic and sintering to ensure that during the processing route the polyurethane template had been replicated accurately with no change to pore shape or distribution. Individual pores were outlined onto overhead transparencies from SEM photomicrographs, which were taken at a magnification that allowed approximately 15–20 full pores to be distinguished clearly. The transparency was then viewed under the image analysis system *Image Pro Plus 4* consisting of a video camera linked directly to the computer's software. Measurements were then taken through the manipulation of the gray scales and use of the ''count'' tool. The equivalent circular diameter (ECD) of the pores were calculated by the image analysis software from the area using the following equation:

$$\mathrm{ECD} = \left(\sqrt{\frac{a}{\pi}}\right)^2$$

where a is the area.

Density

The samples were measured accurately with a micrometer and weighed dry (W_{dry}). The samples were then immersed in a beaker of distilled water and held under vacuum so that the water could penetrate all the macropores. Care was taken to ensure that the minimum amount of ''boiling'' took place under vacuum. The samples were then re-weighed underwater using a Mettler Toledo density kit, to produce the measurement W_{sub}. The samples were then carefully removed from the beaker and dabbed on a wet tissue for 1/2 s to remove any surface water droplets without losing any of the water onto the tissue through capillary action. The samples were then re-weighed in air to produce the measurement W_{sat}. Apparent, bulk and relative densities were calculated using the following calculations. The real density was found through X-ray diffraction (XRD) measurements (see Materials and methods, XRD, below).

$$\text{Apparent density} = \left(\frac{W_{dry}}{W_{sat} - W_{sub}}\right)\rho H_2O$$

$$\text{Relative density} = \frac{\text{Apparent density}}{\text{Real density}}$$

$$\text{Closed porosity} = 1 - \frac{\text{Apparent density}}{\text{Real density}}$$

$$\text{Bulk density} = \frac{W_{dry}}{w \times 1 \times d}$$

where W_{dry} is the weight of dry sample; W_{sat} is the weight of saturated sample; W_{sub} is the weight of submerged sample; w is the width of sample; l is the length of sample; d is the depth of sample and; ρH_2O is the density of water.

X-ray diffraction

To find the real density of the ceramics XRD was carried out on a Phillips PW1050/1082 powder diffractometer, in flat plate geometry using Ni filtered CuK_α radiation (wavelength 1.5409 Å). Samples were ground to a fine powder and mounted in the holder of the diffractometer. Data was collected from 10° to 90°2θ with a step size of 0.02° and a count time of 12 s. The data was refined to find the phase element fractions and density of each phase so that the overall real density of the sample could be found, by multiplying each phase element fraction with its density and then adding the corrected densities together.

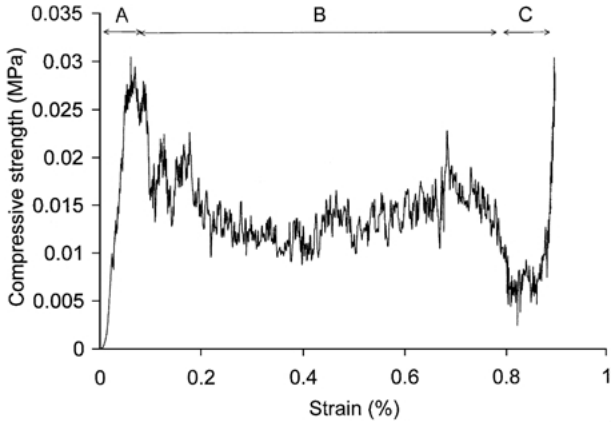

Figure 1 Compression test of a GR-HA foam showing the three regions of strain.

Mechanical testing

Compression testing was performed on a floor standing Instron 4505 using a 1 kN-load cell. Load was applied axially to the sample with a crosshead velocity of $0.06\,\text{mm}\,\text{min}^{-1}$ the test was recorded with a data point every 0.5 s. The ultimate compressive strength (UCS) was defined as the maximum compressive strength obtained during testing before densification (region C on Fig. 1).

Scanning electron microscopy (SEM)

The ceramic foams were sectioned horizontally with a sharp razor blade and mounted onto aluminum SEM stubs with Araldite and left to dry for 24 h. The mounted specimens were then sputter coated with gold and viewed under the SEM (Stereoscan 90, Cambridge Instruments).

Results

Mechanical testing

The compression testing shown in Fig. 1 shows that the ceramic has the three regions of strain characteristic of an elastic brittle foam. Firstly region A, a linear elastic region controlled by the cell wall bending which is followed by B, a plateau controlled by the brittle crushing of the cells and then the final region of densification, C. From Fig. 2 it can be seen that the additional coating of the ceramic after firing greatly enhances the ultimate compressive strength in both the HA alone and the glass reinforced HA.

Density measurements

In Fig. 3 it can be seen that the relationship between the ''dry'' bulk measurement apparent density is linear but not 1 : 1 in ratio. However, the ''dry'' bulk density and the ''wet'' apparent density minus the closed porosity is linear and has a ratio of 1 : 1. It can also be noted that the foams that had only one coating, were in general at the low density end of the data scatter and those that were coated twice at the high density end. Fig. 4 shows that the UCS does depend on the relative density with an increase in UCS with increasing relative density and conforms to the relationships predicted with a R^2 value of 0.7495 the proportionality constant was 8.99. Again the foams with only one coating were confined to the lower end of the

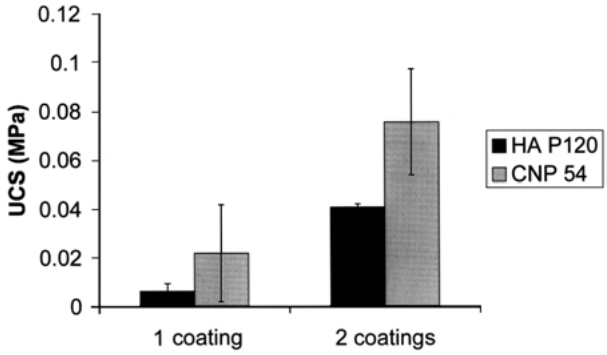

Figure 2 Graph showing mechanical properties of 45 ppi foams coating once and twice with the HA and glass-reinforced HA slips.

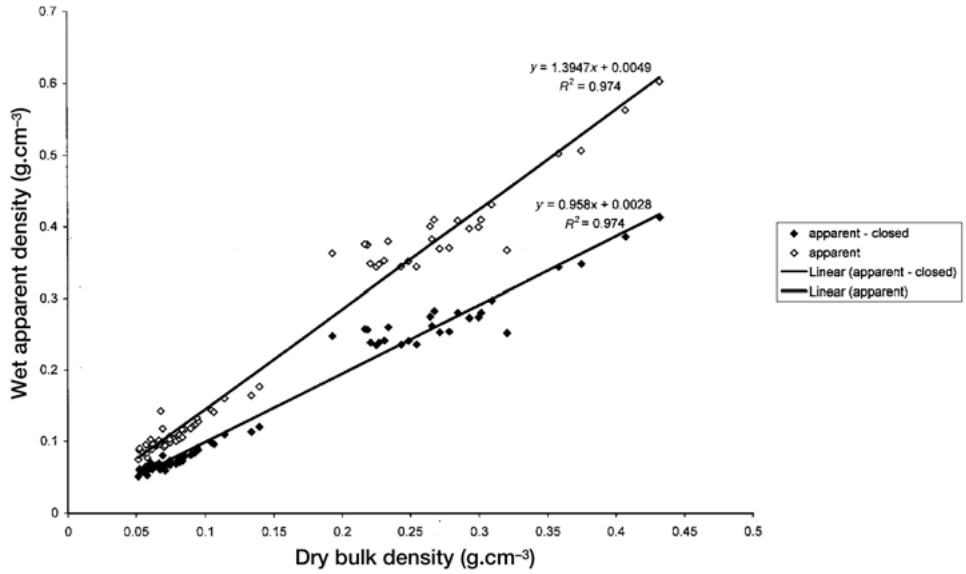

Figure 3 Graph showing the relationships between the ''dry'' bulk density and the corrected ''wet'' apparent density before and after correction. ◆, apparent density minus closed porosity; ◇, apparent density. The open and closed symbols at the lower end of the graph are from once coated specimens and the open and closed symbols at the upper end of the graph are from twice-coated specimens.

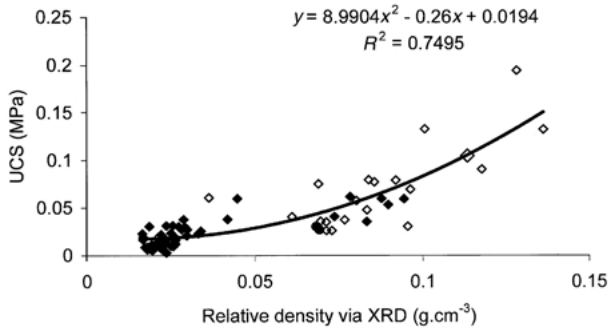

Figure 4 Graph showing quadratic relationship between the relative density and the UCS ◆ one coating of slip ◇ two coatings of slip.

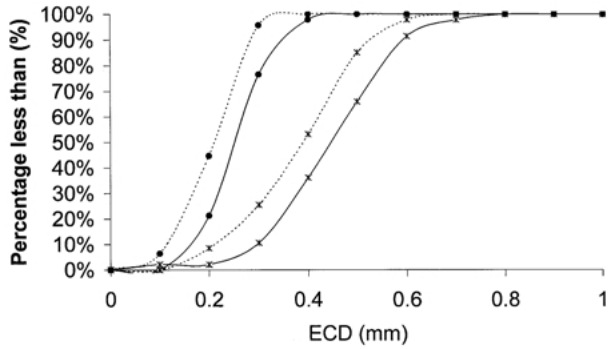

Figure 5 Pore distribution plots from image analysis before and after sintering (— × — 45 ppi polyurethane, before sintering —●— 60 ppi polyurethane, before sintering) (· · · × · · · 45 ppi ceramic, after sintering · · · ● · · · 60 ppi ceramic, after sintering).

density scale and those with two coatings at the high end of the scale.

Image analysis

Fig. 5 shows that during the replication process the distribution of porosity of either foam has not been altered during the replication process. The 45 ppi foam does have a broader distribution than the 60 ppi foam. However, both foams ECD have shrunk during sintering by an average of 0.5 mm

SEM

SEM micrographs Fig. 6(a)–(c) show that the foams have an open reticulated structure after sintering, however, it was found that in some of the higher density specimens had some of the pores were clogged or closed and in the foams coated just once voids were seen to be present within the ceramic struts.

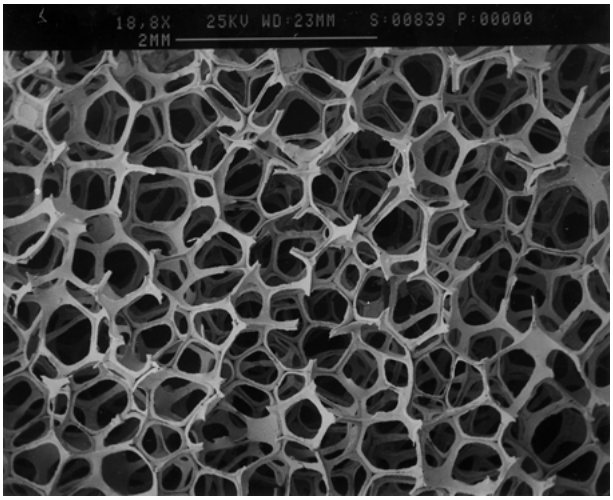

(a)

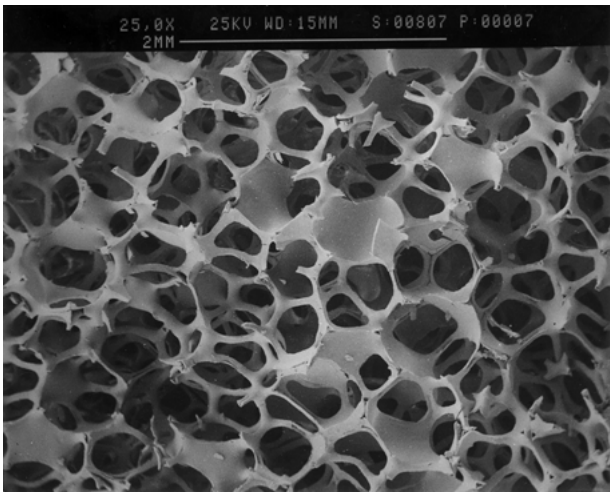

(b)

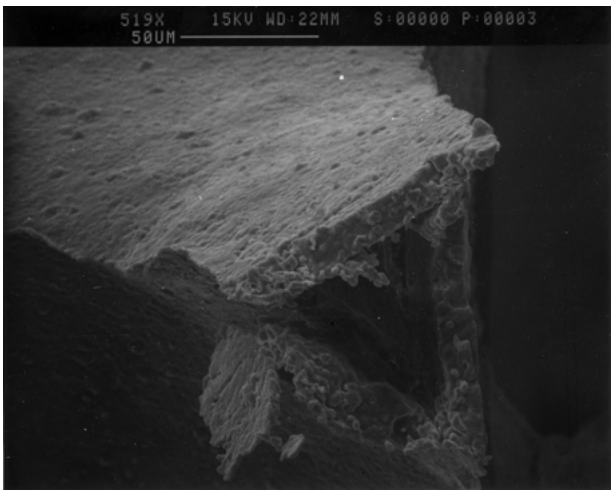

(c)

Figure 6 (a) SEM of a 60 ppi foam; (b) SEM of a 60 ppi foam with some clogged pores; (c) SEM showing voids within the struts of ceramic.

Discussion

Mechanical testing and density

Cells in a porous structure can either be open (comprising of a network of rods) or closed (comprising of a network of plates) [9], isotropic or aniostropic and behavior during compression is dependant on these parameters.

During compression testing there was a region of linear elasticity, controled by cell bending, followed by a linear region, which is controled by the brittle crushing of the cell walls, finally when the cell walls collapse further strain compresses the solid wall itself creating the last region of densification indicating that the material is failing in an elastic brittle manner, characteristic of an open cell ceramic structure [9]. Also the relationship between the porous ceramics relative density and its ultimate compressive strength was best described by a quadratic relationship as described by Gibson and Ashby

[9] for a typical isotropic, open celled material. Deviations from this model could be explained by the appearance of some clogged or closed cells at the higher relative density values that were seen in the SEM micrographs (Fig. 6(b)).

It has been shown in previous research that the measurements of bulk and apparent density should be equal [11]. However, it was found in this work that the bulk density was significantly lower than the apparent density. This is because, when measuring the underwater W_{sub} value for the apparent density calculation the water cannot penetrate the voids that are present within the struts of the ceramic as seen in the SEM micrographs (Fig. 6(c)) therefore making the apparent density appear more dense than it actually is. If the closed porosity is subtracted from the apparent density and then plotted against the bulk density this results in a linear 1 : 1 ratio relationship.

Image analysis

It can be seen from the image analysis data collected that the structure of the polyurethane template has been conserved during the processing procedure and that the pore distribution remains the same. However the actual pore size has decreased by approximately 0.5 mm during sintering which is expected.

Conclusions

From the compression testing results it can be seen that the materials exhibit properties typical of isotropic open cellular foams and that using a glass and also coating the ceramic foams twice significantly enhances their densities and mechanical properties. Image analysis confirms that there is no degradation of the macro-structure when replicating ceramic from the initial polyurethane template.

Acknowledgments

The authors would like to acknowledge the financial support of the Engineering and Physical Sciences Research Council (EPSRC).

References

1. K. A. HING, I. R. GIBSON, J. C. MERRY, I. DI SILVIO, S. M. BEST, P. A. REVELL, W. BONFIELD (1 page abstract), *Trans World Biomater. Cong. 2000*, 440.
2. G. S. JOHNSON, M. R. MUCALO and M. A. LORIER, *J. Mater. Sci.: Mater. Med.* **11** (2000) 427–441.
3. D. M. ROY, *Nature* **247** (1974) 220–222.
4. D. M. LIU, *J. Mater. Sci.: Mater. Med.* **8** (1997) 227–232.
5. J. G. P. BINNER and J. REICHERT, *J. Mater. Sci.* **31** (1996) 5717–5723.
6. M. FABBRI, G. C. CELOTTI and A. RAVAGLIOLI, *Biomaterials* **16** (1995) 225–228.
7. J. C. KNOWLES, S. CALLCUT and G. GEORGIOU, *ibid.* **21** (2000) 1387–1392.
8. K. A. HING, S. M. BEST, K. E. TANNER and W. BONFIELD, *J. Mater. Sci.: Mater Med.* **10** (1999) 663–670.
9. L. J. GIBSON and M. F. ASHBY, ''Cellular Solids'', 2nd edn. (Cambridge University Press, Cambridge, 1997).
10. W. J. WHITEHOUSE and E. D. DYSON, *J. Anatomy* **118** (1974) 417–444.
11. K. A. HING, ''Assessment of Porous Hydroxyapatite for Bone Replacement'' Ph.D. Thesis (University of London, 1996).

Received 16 July
and accepted 21 September 2001